Journal of Building Engineering 84 (2024) 108476

Contents lists available at ScienceDirect

Journal of Building Engineering

journal homepage: www.elsevier.com/locate/jobe

Advancing service life estimation of reinforced concrete considering the coupling effects of multiple factors: Hybridized physical testing and machine learning approach

Xuanrui Yu [a], Jiehong Li [b,*], Yang Yu [b], Anxiang Song [c]

[a] School of Civil Engineering, Chongqing University of Science and Technology, Shapingba District, Chongqing 401331, People's Republic of China
[b] Centre for Infrastructural Engineering and Safety, School of Civil and Environmental Engineering, The University of New South Wales, High Street, Sydney 2052, Australia
[c] School of Civil Engineering, Chongqing Jiao Tong University, Nan an District, Chongqing 400074, People's Republic of China

ARTICLE INFO

Keywords:
Chloride-induced corrosion
Reinforced concrete structures
Fick's second law
The service life
Machine learning approaches

ABSTRACT

Chloride-induced corrosion is the primary factor that significantly impacts the service life of reinforced concrete structures. Therefore, it is crucial to investigate the transportation behavior of chloride ions within concrete structures to accurately estimate their service life. Previous studies have mostly examined the diffusion of chloride ions through physical tests on concrete specimens. Some data-driven models have also been developed to predict the chloride ion concentration at different depths in concrete structures. However, these prediction models often considered random factors in materials and the environment separately, neglecting their coupled effects. As a result, there can be a significant disparity between the predicted results and the actual test outcomes. To achieve a more precise evaluation of the service life, this study conducted a physical test to investigate the diffusion behavior of chloride ions in plain concrete specimens. Factors such as water-cement ratio (W/C), coarse aggregate volume fraction (v) (ratios of the mass of coarse aggregates to the total mass of concrete specimen), ratios of environmental temperature to maintenance standard temperature (T/T_0), ratios of environmental humidity to maintenance humidity (h/h_0), and ratios of exposure time to maintenance time (t/t_0) were considered in the test. Based on the test results, machine learning approaches were employed to determine the influence of each factor on the chloride diffusion coefficient (D) and surface chloride concentration (C_s). Subsequently, a prediction model was developed using the second Fick's law, with the chloride ion concentration at each depth as the output and the aforementioned factors as the inputs. Furthermore, by analyzing the above results, the study examined the impacts of various factors on the service life of reinforced concrete structures. The findings indicate that W/C and v are the most significant factors affecting D and C_s. As W/C and T/T_0 increase, both D and C_s also increase. Conversely, the volume fraction of coarse aggregate has a hindering effect on the diffusion of chloride ions in concrete structures. Additionally, the study explored the effect of each input factor on the service life of reinforced concrete structures considering the effect of the above factors. Overall, these findings provide valuable insights into improving the accuracy of estimating the service life of reinforced concrete structures by considering the coupled effects of materials and environmental factors.

* Corresponding author.
E-mail address: jiehong.li@unsw.edu.au (J. Li).

https://doi.org/10.1016/j.jobe.2024.108476
Received 20 July 2023; Received in revised form 27 December 2023; Accepted 6 January 2024
Available online 14 January 2024

1. Introduction

Reinforced concrete structures that are exposed to the environment are prone to corrosion caused by chloride ions. This chloride-induced corrosion has significant economic and safety implications [1–3]. Previous studies have revealed that approximately 80 % of fatigue cracks in concrete structures are a result of corrosion damage [4]. The uncertainty and impact of corrosion damage on the service life of reinforced concrete structures pose significant challenges. Currently, there is a lack of specific codes or guidelines to address this issue. Therefore, it is of utmost importance to establish a model that can investigate the diffusion behavior of chloride ions within concrete structures. Such a model would greatly contribute to the evaluation of the service life of these structures. By understanding the diffusion law of chloride ions, it becomes possible to assess the potential for corrosion-related deterioration accurately.

To investigate the diffusion behavior of chloride ions in plain concrete structures, several tests have been conducted by researchers. Thomas [5] proposed a theoretical model based on the second Fick's law to study the diffusion mechanism of chloride ions in concrete structures. The results revealed a decreasing trend in chloride ion concentration as the diffusion depth increased. Collepardi [6] performed tests to explore the diffusion law of chloride ions in plain concrete specimens and developed a prediction model based on the findings. However, this model did not consider the time-dependent effect of the chloride diffusion coefficient. Moreover, Zheng [7] conducted physical tests to examine the diffusion of chloride ions and obtained values for the chloride diffusion coefficient (D) and surface chloride concentration (C_s) at different exposure times. Using Fick's second law, an empirical model was established to estimate the chloride ion concentration at various depths in concrete specimens. In addition, Wang [8–12] conducted tests and observed that the coarse aggregate volume fraction (v) had a significant impact on D and C_s. Specifically, as the volume fraction of coarse aggregate increased, both D and C_s decreased. This implies that increasing the volume fraction of coarse aggregate appropriately can enhance the durability of reinforced concrete structures. Furthermore, Suryavanshi [13] investigated the diffusion mechanism of chloride ions and found that the chloride diffusion coefficient increased with an increase in the water-cement ratio (W/C). At the same time, Ren [14] analyzed the durability of concrete structures with different water-cement ratios, considering the impact of chloride-induced corrosion, and developed a model to estimate their service life.

Moreover, several tests have been conducted to investigate the diffusion mechanism of chloride ions in concrete structures, taking into account various random factors in the environment. For instance, Liu et al. [15] conducted a test to examine the impact of temperature on the chloride diffusivity of concrete. Their findings revealed that an increase in temperature accelerates the diffusion of chloride ions in concrete structures. Additionally, El Hassan [16,17] investigated the effect of climatic conditions on chloride ion diffusion in concrete structures. The results demonstrated that both humidity and temperature have a significant influence on the chloride ions diffusion coefficient.

Furthermore, with the advancement of computer technology, machine learning methods are gradually being applied in engineering structures. Hodhod [18] developed an artificial neural network model to assess chloride ion diffusivity in high-performance concrete. Kim Y [19] established a neural network model and proposed an assessment method for the apparent diffusion coefficient of chloride ions in complex environments. They analyzed the influence of environmental factors such as temperature and humidity. Al-samawi M [20] developed a cellular automaton model, separately considering the effects of relative environmental humidity and temperature variations on the diffusion patterns of chloride ions. Song HW [21] used a neural network algorithm to assess the chloride ion permeability in high-performance concrete. Kim et al. [22] utilized a backpropagation (BP) neural network model to study the diffusion behavior of chloride ions in concrete structures. Similarly, T Gupta [23] analyzed the time-dependent pattern of chloride ion diffusion rates using an artificial neural network model, taking into account the temperature's impact on the chloride ion diffusion coefficient and revealing the impact of the environment on its durability.

From the previous analysis, it is evident that several studies have conducted tests to examine the diffusion behavior of chloride ions in concrete structures and proposed prediction models for estimating chloride ion concentrations at different depths. However, most of these studies have only considered the effects of individual factors in isolation, neglecting their coupled effects. As a result, accurately estimating the service life of concrete structures using these models becomes challenging. Therefore, the primary objective of this study is to comprehensively investigate the diffusion of chloride ions in concrete structures by considering the coupled effects of several factors in both materials and the environment such as the water-cement ratio, environment temperature, environment humidity and coarse aggregate volume fraction. To achieve this, a total of 118 specimens with the dimension of 150 cm × 150 cm × 450 cm were designed and manufactured. Placing these specimens in the environmental test chamber, which is specifically designed to simulate and control various environmental conditions, enables automatic control of factors such as temperature, humidity, salt spray, acid rain, and load. After the specimens have undergone corrosion for the appropriate duration within the environmental test chamber, these specimens were then used to conduct tests to analyze the diffusion law of chloride ions within concrete structures. The influence of each factor on the surface chloride concentration (C_s) and chloride diffusion coefficient (D) was thoroughly analyzed. Based on Fick's second law, a model was established to estimate the chloride ion concentration at various depths in concrete structures. In this model, the chloride ion concentration at each depth served as the output, while the aforementioned factors were considered as inputs. Furthermore, the study analyzed the service life of reinforced concrete structures using the developed model and comprehensive analysis of chloride ion diffusion. By incorporating the coupled effects of various factors, a more accurate assessment of the service life of concrete structures can be achieved.

1.1. Research significance

Compared with the existing published materials, this paper carried out artificial accelerated corrosion test for reinforced concrete structures, considering the influence of environmental factors and material factors on chloride ion diffusion coefficient and surface chloride ion concentration. Based on Fick 's second law, a model was established to reveal the diffusion mechanism of chloride ions

under different environmental conditions. The service life of reinforced concrete structures is evaluated, and the significant influence of each input variable on its service life is analyzed, which effectively solves a major gap in the existing theoretical research. The objective of this study is to provide a comprehensive approach that aids engineers and researchers in gaining a better understanding of the impact of corrosion on the service life of reinforced concrete structures. Through the establishment of this theoretical model, the corrosion behavior of reinforced concrete structures can be predicted more accurately, which provides strong support for engineering-related design and maintenance work.

2. Methodology and experimental studies

By conducting accelerated corrosion tests, we simulated the erosion process of chloride ions on concrete structures. By testing the chloride ion concentration in the interlayer of concrete under different conditions, we revealed the transmission patterns of chloride ions in concrete structures under multiple coupled effects. Additionally, we analyzed the influence of environmental temperature, humidity, coarse aggregate volume fraction, and exposure time on the transmission patterns of chloride ions of concrete structures.

2.1. Material properties

The specimens were cast using Ordinary Portland cement (P·O.42.5) produced by the Chong-Qin Cement Plant. The cement had a density of 3100 kg/m^3. Table 1 presents the significant components of cement. For the aggregates, river sand and natural crushed limestone with continuous grading were utilized as the fine and coarse aggregates, respectively. The apparent density of the river sand was 2700 kg/m^3, while the natural crushed limestone had an apparent density of 2600 kg/m^3. The coarse aggregate had a nominal size range of 6–20 mm [23]. Before casting, all the raw coarse aggregate was pre-wet and saturated with distilled water. The casting and curing of the specimens were carried out using distilled water as well. Table 2 provides partial mixed proportions of the concrete specimens, where the coarse aggregate volume fraction (by mass) ranged from 0.2 to 0.6 [8,9], and the water-cement ratio (*W/C*) ranged from 0.3 to 0.6.

2.2. Casting process of specimens

A total of 118 specimens measuring 150 cm × 150 cm × 450 cm were designed and manufactured using plastic molds, as depicted in Fig. 1. The thickness of concrete cover is 20 mm [8,9]. After compaction on a vibration table, all specimens were transferred to an environment with a temperature of 20 °C and a humidity of 75 % [8,9] (as shown in Fig. 2). They were then cured using a calcium hydroxide ($Ca(OH)_2$) solution. The workability of each concrete mix was determined using the slump test, which helped assess the consistency and flowability of the concrete mixture.

2.3. Experimental environment

The temperature of the testing chamber ranges from 25 °C to 40 °C, while the humidity ranges from 75 % to 95 %. This controlled environment simulated varying climatic conditions that concrete structures may encounter in real-world scenarios. Additionally, the exposure time for the concrete specimens ranged from 35 days to 235 days. To ensure the highest experimental precision while maximizing the conservation of concrete material, this study designed the corresponding orthogonal experiments. To simulate a marine environment, 3.5 % NaCl (sodium chloride) solution was utilized [8]. During the testing process, the saltwater solution was changed once a week to maintain a constant concentration of chloride ions. For the corrosion testing, the experiments were conducted in an environmental test chamber with automatic temperature and humidity control. The NaCl solution was evenly sprayed from a nozzle, ensuring that the specimens were fully exposed to corrosive chloride ions, (as shown in Fig. 3). It is important to note that this study focused on investigating the diffusion of chloride ions in concrete structures from one dimension. This is considered an initial step in exploring the durability of reinforced concrete structures. To control the exposure of the specimens to chloride ions, a protective coating consisting of an epoxy polyurethane-based sealant was applied to seal the five sides of the specimens. This coating effectively prevented chloride ions from entering through these sealed surfaces, while leaving one surface exposed to the chloride ions environment.

2.4. Testing the chloride ions concentration at each depth

After each specimen was corroded for 35, 65, 100, 140, 175, 200, and 235 days, the corresponding specimens were taken out of the test chamber and uniformly divided into three parts, labeled as I to III. Part I was considered the representative segment used for drilling concrete powders, as shown in Fig. 4. Concrete powders were obtained by drilling along the x-axis direction for each hole at

Table 1
Properties of ordinary Portland cement, OPC (P·O.42.5).

Properties Chemical analyzes (%)	Cement
Chemical analyzes (%)	
Calcium oxide (Cao)	62.5
Silicon dioxide (SiO_2)	20.5
Ferric oxide (Fe_2O_3)	5.50
Aluminum oxide (Al_2O_3)	5.85
Magnesium oxide (MgO)	1.93
Sulfur trioxide (SO_3)	2.15

Table 2
Mix proportion of concrete specimens (Kg/m^3).

Type	Cement	Water	Fine aggregate	Coarse aggregate
CS-1	565	171	1188	480
CS-2	496	198	1229	480
CS-3	431	215	1277	480
CS-4	413	247	1263	480
CS-5	565	171	1054	613
CS-6	496	198	388	961
CS-7	431	215	196	1201
CS-8	413	247	58	1441

Fig. 1. The concrete specimens.

different positions. Subsequently, the concrete powders from each drilled hole were dissolved in pure water. Finally, the free chloride ion concentration in the solution was measured using a chloride ion meter (BION1881), and the test results were displayed in Fig. 5. The part I of the specimens was considered the experimental group, and the chloride ion concentration test results were used in Eq (1) to establish the corresponding predictive model for predicting chloride ion concentrations in various layers of concrete. The chloride ion concentration test results of Part II and Part III were considered the control group, utilized to verify the model's accuracy.

3. Results and discussion

3.1. Chloride ions diffusion

The chloride profiles against diffusion depths in plain concrete specimens, corresponding to different exposure times, are presented in Fig. 6. The red dots in the figure represent the chloride ion concentration at each depth. In concrete structures. The blue dashed line is obtained by fitting the red dots, aiming to describe the distribution pattern of chloride ions in concrete. It is worth noting that the figures in this study are all presented as a percentage of the concrete mass (%). From the previous analysis, it is evident that the concentration of chloride ions decreases as the diffusion depth increases within the concrete specimens. Additionally, the exposure time has a positive effect on the diffusion of chloride ions. However, as the diffusion depth increases, the influence of exposure time on chloride ion diffusion diminishes. These trends in chloride profiles are consistent with the findings reported in previous literature [24, 25].

Fig. 7(a)-(d) respectively demonstrate the effects of environmental temperature, humidity, and the volume fraction of coarse aggregate on the distribution pattern of chloride ion concentration. The results show that as the volume fraction of coarse aggregate increases, the chloride ion concentration among the various layers of concrete decreases, thus impeding the diffusion of chloride ions to some extent. Conversely, an increase in the water-cement ratio, environmental temperature, and humidity facilitates the diffusion of chloride ions in concrete structures.

3.2. A prediction model for estimating the chloride ions concentration at each depth

In this section, a prediction model based on Fick's second law was proposed to estimate the concentration of chloride ions at various depths within concrete structures. This model provides insights into the diffusion mechanism of chloride ions and enables the assessment of their concentration profiles. By understanding the diffusion behavior of chloride ions, it becomes possible to predict the

Fig. 2. The maintenance chamber.

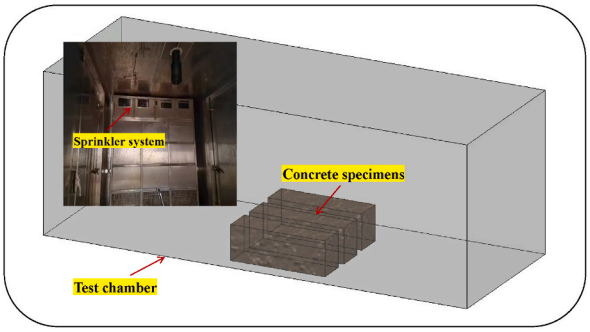

Fig. 3. Test chamber.

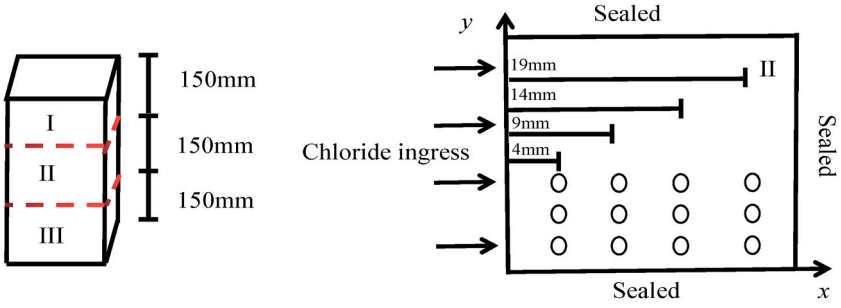

Fig. 4. Sample holes distribution of specimens.

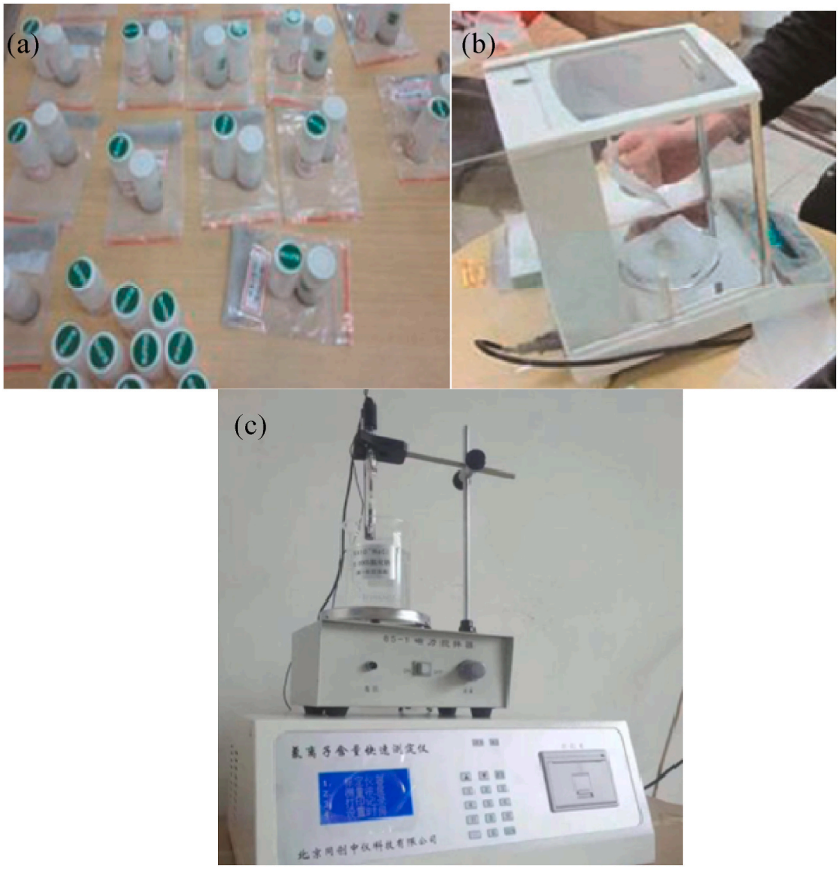

Fig. 5. Chlorine ion concentration measurement process(a) the concrete powder (b) weighing the powder(c) test the chloride ions.

service life of structures and enhance their durability performance. This research significantly contributes to the advancement of knowledge in the field and lays a solid foundation for improving the longevity of structures.

3.2.1. Fick's second law

When concrete structures are exposed to harsh environments, the ingress of chloride ions can occur through multiple mechanisms, including diffusion, convection, permeation, and the surface deposition of airborne salts. However, based on previous studies [23], it has been established that diffusion is the primary mechanism through which chloride ions penetrate concrete structures. Therefore, this section will primarily focus on the process of establishing a model for predicting chloride ion diffusion in concrete structures. The following criteria were applied in constructing the prediction model.

(1) The model solely investigated the diffusion mechanism of chloride ions and did not consider the effects of other mechanisms such as convection and permeation.
(2) The diffusion of chloride ions should be a three-dimensional spatial process, and ideally, a three-dimensional diffusion model should be established to describe the diffusion pattern of chloride ions in concrete structures. However, due to the limitations of testing equipment, it is currently not feasible to experimentally measure the chloride ion concentrations at various locations within concrete structures. The majority of studies have still only explored the diffusion behavior of chloride ions in one direction [8,9]. To verify the accuracy of the one-dimensional diffusion model, Wu [24] and others compared the differences between one-dimensional and two-dimensional diffusion models and found that the relative error in the predicted results of both was within 12 %, indirectly demonstrating the reliability of the one-dimensional diffusion model. Therefore, this paper also focused on exploring chloride ion diffusion in one direction, emphasizing the study of the influence of coupled environmental and material factors on its diffusion behavior.
(3) The investigation specifically examined the diffusion of chloride ions in plain concrete structures, without considering the blocking effect of steel bars.

The Fick's second law was often used to illustrate the transport mechanism of chloride ions in concrete structures, which can be expressed as follows [23,24].

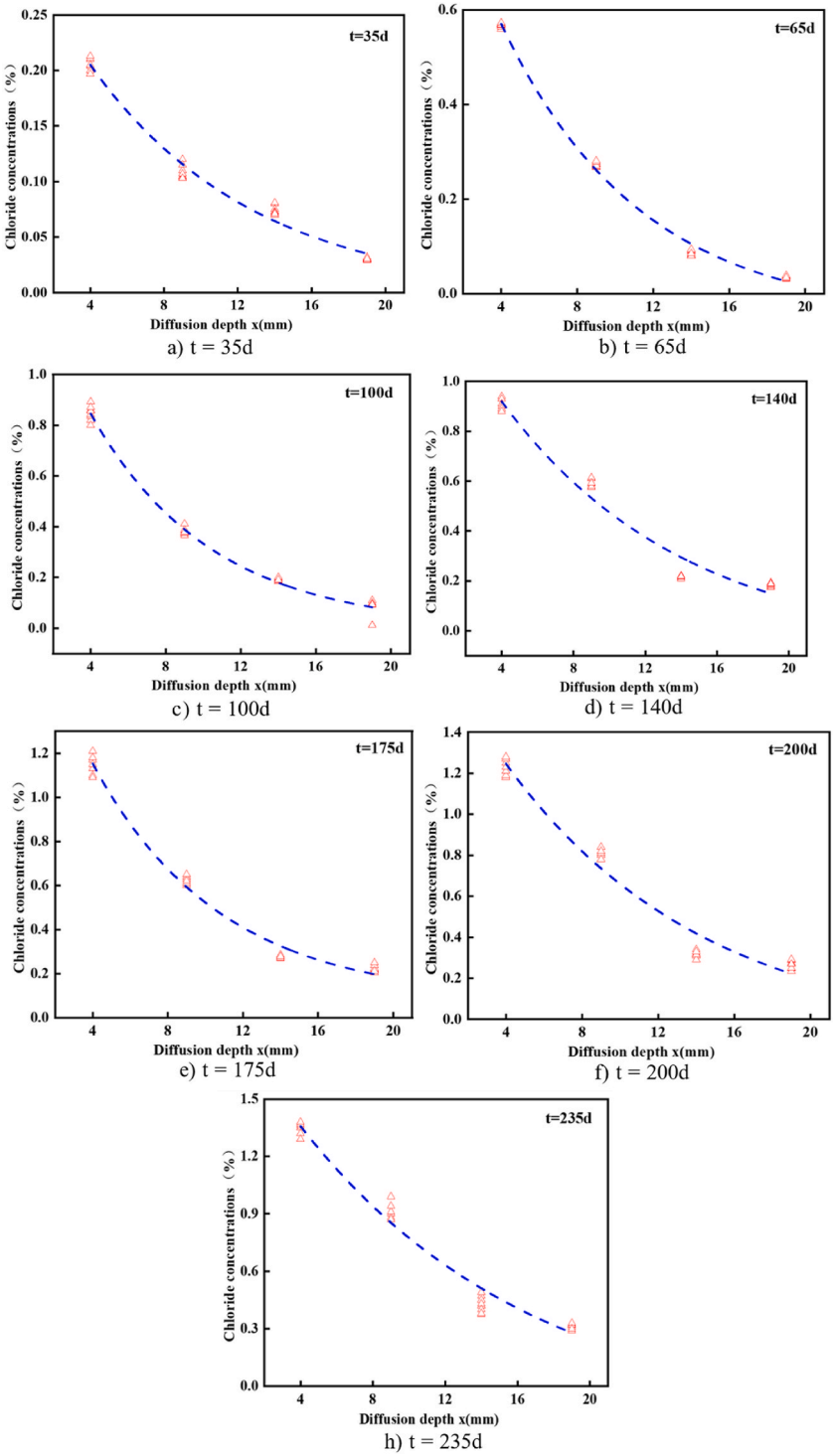

Fig. 6. Chloride ions concentration at each depth in concrete structures.

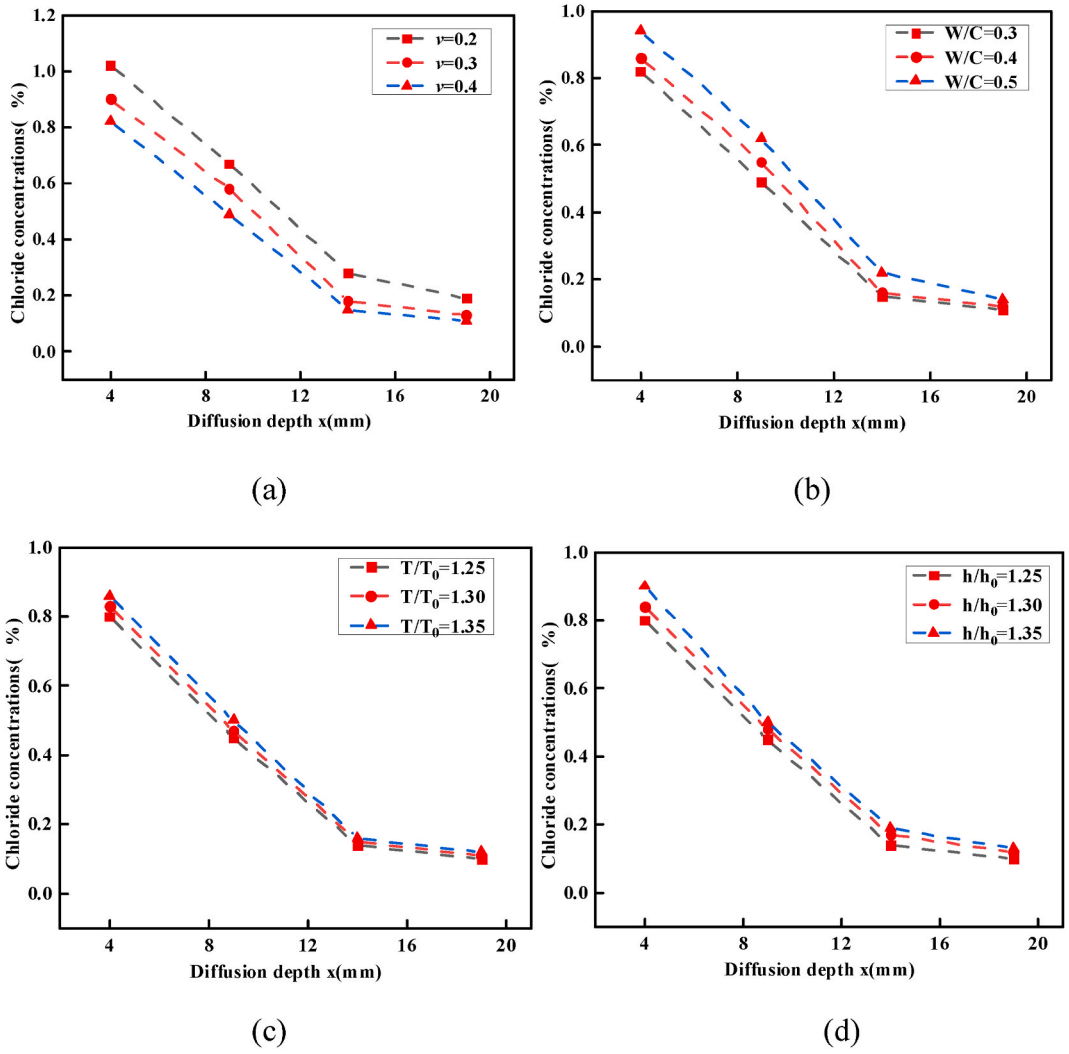

Fig. 7. The impact of each input variable on chloride ion concentration. (a)ν (b)W/C (c)T/T_0 (d) h/h_0.

$$C(x,t) = C_s\left(1 - erf\frac{x}{2\sqrt{D \times t}}\right) \tag{1}$$

Where: $C(x,t)$ denotes the chloride ions concentration at each depth (%), where t means the exposure time and x means the diffusion depth. D stands for the apparent chloride diffusion coefficient, C_s means the surface chloride ions concentration. $erf(x)$ means the error function, the specific expression is shown in Eq. (2), which can be solved by the least square method.

$$erf(x) = \frac{2}{\sqrt{\pi}} \times \int_0^z \exp(\beta^2) d\beta \tag{2}$$

3.2.2. *The calculation process of C_s and D*

Based on Eq. (1), D and C_s can be obtained by fitting the experimental measurements (as shown in Fig. 6), the calculated results are shown in Figs. 8 and 9. Figs. 8 and 9 present the time-varying behavior of the chloride ion diffusion coefficient and the surface chloride ion concentration, respectively. The results indicate certain trends and relationships among the variables. The results show that the chloride ion diffusion coefficient and the surface chloride ion concentration demonstrate an increase as the water-cement ratio (W/C), the ratio of environmental temperature to maintenance standard temperature (T/T_0). Conversely, they exhibit a decrease with an increase in the coarse aggregate volume fraction (ν). Furthermore, the exposure time ratio (t/t_0) has a significant impact on both the chloride ion diffusion coefficient and the surface chloride ion concentration. Specifically, the exposure time ratio (t/t_0) shows a negative correlation with the chloride ion diffusion coefficient, meaning that a longer exposure time leads to a decrease in the diffusion coefficient. On the other hand, the exposure time ratio (t/t_0) exhibits a positive correlation with the surface chloride ion concentration. In addition, the chloride ion diffusion coefficient and the surface chloride ion concentration are also affected by the h/h_0. Higher

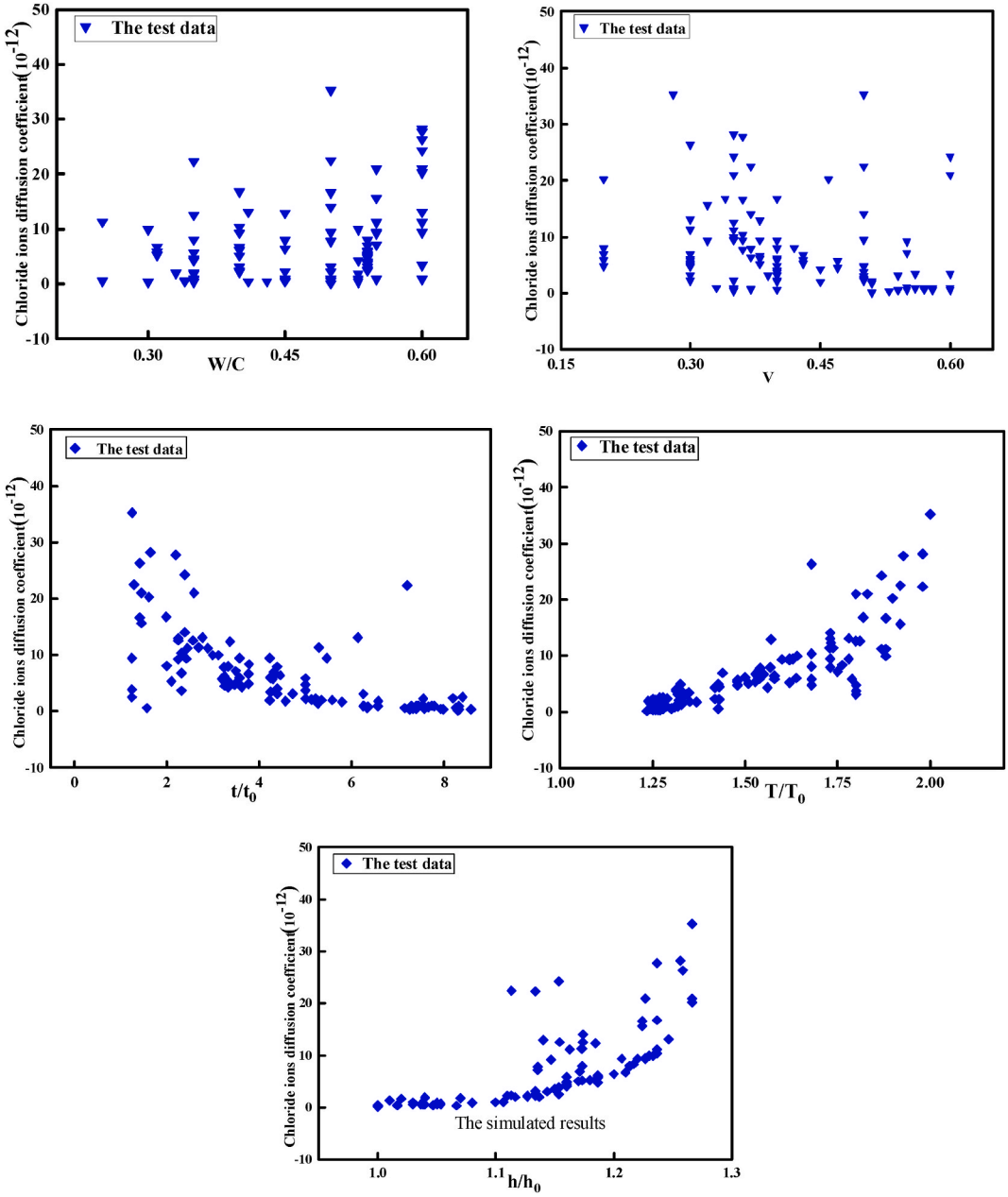

Fig. 8. The results of the diffusion coefficient.

humidity can increase the moisture content in concrete and maintain a higher moisture level within the concrete. This leads to an accelerated diffusion rate of chloride ions in the concrete, thereby increasing the chloride ion diffusion coefficient and decreasing the surface chloride ion concentration.

Based on the analysis above, it can be concluded that the diffusion coefficient of chloride ions and the surface chloride ion concentration in concrete structures are influenced by various random factors from both the material and the environment. Conventional methods for estimating these parameters, such as statistical analysis, can ensure accuracy to some extent. However, machine learning approaches are considered more advanced and capable of effectively addressing complex nonlinear problems. In order to explore the impact of these factors, six machine learning approaches were employed: backpropagation neural network (BPNN), decision tree (DT), random forest (RF), linear regression (LR), ridge regression (RR), and K-Nearest Neighbor model (KNN). Each model's calculation process is illustrated in Fig. 10. Backpropagation Neural Network (BPNN) is a neural network model based on the backpropagation algorithm [25]. It consists of multiple neurons organized in a hierarchical structure, and it learns the relationship between input and output by continuously adjusting connection weights. BPNN can be used for regression and classification tasks and optimizes the model

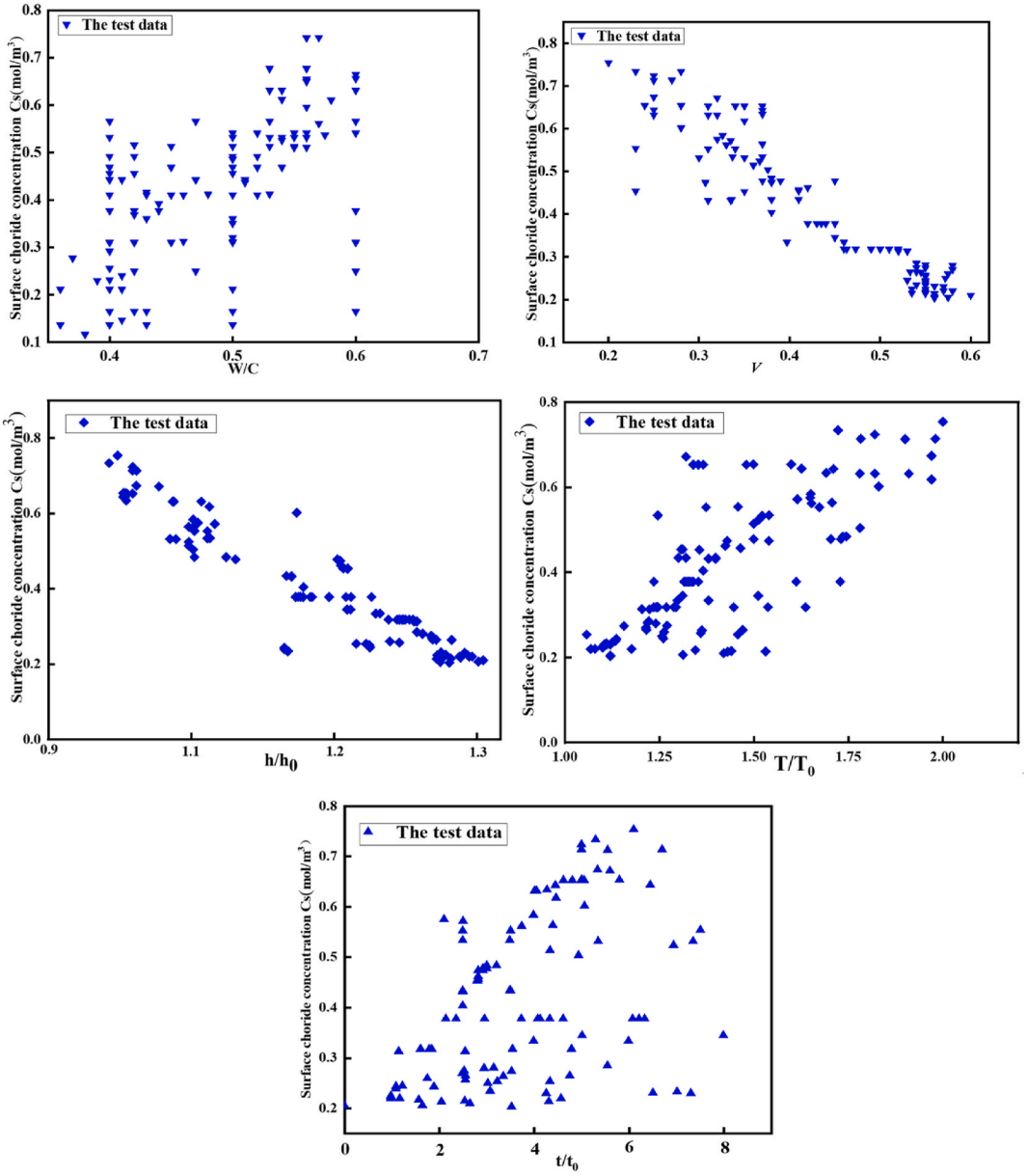

Fig. 9. The results of the surface chloride ions.

by calculating errors during the training process. Decision Tree (DT) is a tree-based model used for classification and regression. It partitions input features in a step-by-step manner, creating a tree-like structure where each leaf node represents a class or value. The decision tree model learns patterns in the data to make predictions and is known for its interpretability and simplicity [25]. Random Forest (RF) is an ensemble learning method composed of multiple decision trees. Each decision tree in the random forest is trained using random subsets of data and features. The final prediction is made by aggregating the results from individual trees through voting or averaging. Random Forest exhibits good generalization and robustness against overfitting [24]. Linear Regression (LR) is a basic regression model used to establish a linear relationship between input features and output. It assumes a linear correlation between the input features and the output and fits the best linear model by minimizing the error between predicted and actual values. Ridge Regression (RR): is an improvement over linear regression that introduces a regularization term to control the model's complexity. The regularization term restricts the size of the model parameters, preventing overfitting and enhancing the model's generalization capability. K-Nearest Neighbor model (KNN) model is an instance-based learning method. It finds the K nearest neighbors to a target sample based on the similarity of input features and predicts the target sample's class or value through voting or averaging. KNN is simple and easy to understand, but it may have high computational complexity when dealing with large datasets.

The BP model with two hidden layers were applied using a random test-train split of the database, The hyperbolic tangent function

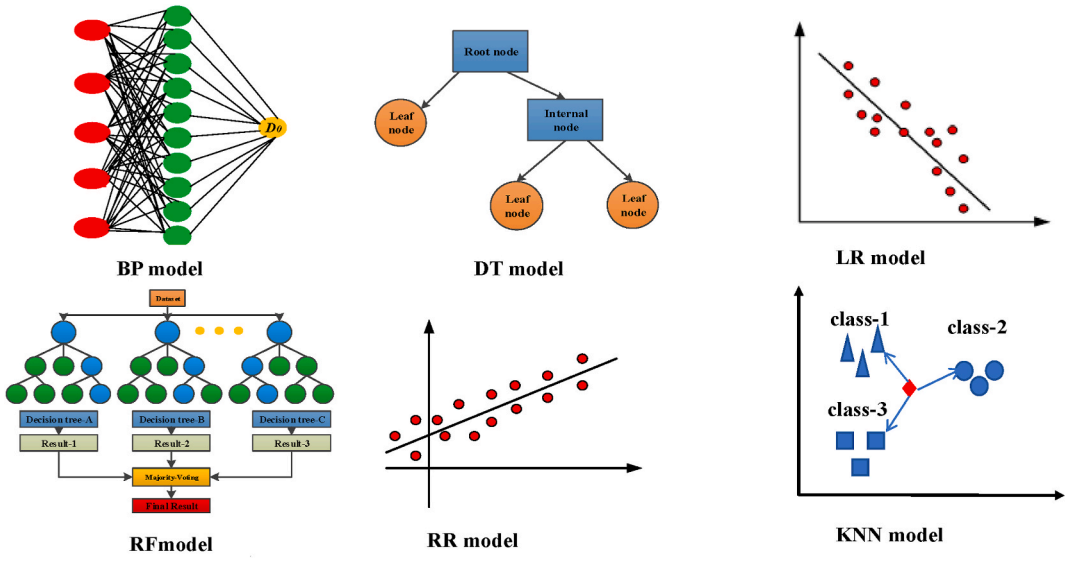

Fig. 10. Graphical representation of the ML algorithms.

was chosen as the activation function. In addition, the number of neurons in the hidden layer significantly impacts the accuracy of the prediction model. To determine the appropriate number of neurons, these algorithms leverage their research capabilities to identify the optimal number of neurons for the hidden layer. The number of neurons in the hidden layer can be obtained as follows:

$$H = \sqrt{I + Q} + B \tag{3}$$

Where: H means the number of neurons in the hidden layer, I means the number of neurons in the input layer, Q stands for the number of neurons in the output layer, and A takes an integer between 1 and 10. To account for the potential issues of overfitting (excessive complexity leading to poor generalization) and underfitting (insufficient complexity leading to inadequate modeling), the number of neurons in the hidden layer is set to ten. This value is determined through repeated debugging and experimentation conducted in the research paper. The decision tree model has a maximum depth of 10 and a minimum samples leaf of three. The random forest model has 100 base estimators, with tree parameters matching those of the decision tree model. The KNN model utilizes the Euclidean distance as its distance metric and employs distance-weighted strategy. The other two common models are not elaborated here but can be referenced from literature [25]. Following a specific methodology. The database, represented by Figs. 8 and 9, was divided into two subsets: a training subset and a testing subset. The split was performed randomly, with 70 % of the data (86 samples) assigned to the training subset and 30 % (35 samples) to the testing subset [25]. The process involved multiple steps. Initially, the database was divided into several groups. Then, these groups were further divided randomly using the random function in MATLAB. Through this process, the training set and test set were selected by random sampling. The inputs for the models included random factors such as (W/C), (T/T_0), (h/h_0), v and (t/t_0), while C_s and D were considered as the outputs to be predicted. To ensure the accuracy of the results, 10-fold cross-validation was applied to all models. This entailed dividing the dataset into 10 subsets, and the models were trained and tested 10 times, with each subset serving as the testing set once.

The performance of each model was evaluated using various indicators, including the correlation coefficient (R), mean absolute error (MAE), root mean square error (RMSE) and mean absolute percentage error (*MAPE*), as shown in Table 3.

The coefficient of determination R^2 is a measure of how well the established model can estimate the test results. A higher value of R^2 indicates a better predictor model. R^2 ranges from 0 to 1, where 1 represents a perfect fit of the model to the data. Additionally, the root

Table 3
The performance of each indicator [22].

Name of the indicators	Notation	Expression
Coefficient of determination	R^2	$R^2 = \frac{[\sum_{i=1}^{n}(y-\overline{y})(y'-\overline{y'})]^2}{\sum_{i=1}^{n}(y-\overline{y})^2\sum_{i=1}^{n}(y'-\overline{y'})^2}$
Root mean square error	*RMSE*	$RMSE = \sqrt{\frac{1}{n}\sum_{i=1}^{n}(y-y')^2}$
Mean absolute error	*MAE*	$MAE = \frac{1}{n}\sum_{i=1}^{n}(y-y')$
Mean absolute percentage error	*MAPE*	$MAPE = \frac{1}{n}\sum_{1}^{n}\frac{y-y'}{y}\times 100\%$

Notes: Where y' means the predicted consequences, y means the test results and n = number of samples.

Table 4
The evaluation results of each data-driven model.

(ML) models	R^2	*RMSE*	*MAE*	*MAPE*
BP model	0.874	0.835	0.984	9.3 %
Decision tree model	0.708	1.301	1.443	19.7 %
Random forest model	0.804	0.974	1.032	10.9 %
Linear regression	0.608	1.458	1.632	27.3 %
Ridge regression model	0.784	1.182	1.278	15.2 %
KNN Model	0.712	1.233	1.534	23.2 %

mean square error (*RMSE*), mean absolute error (*MAE*) and mean absolute percentage error are commonly used to evaluate the performance of regression models. A lower *RMSE* and *MAE* indicate better predictive accuracy. Therefore, in summary, a good predictor model is characterized by a higher value of R^2, indicating a better fit to the data, and lower values of *RMSE* and *MAE*, indicating more accurate predictions.

Compared with the test results, the evaluation results of each data-driven model were show in Table 4. It can be seen that the BP neural network model with the highest R^2 (0.874) and the lowest *RMSE* (0.835), which can simulate the D and C_s well. Similarly, the value of R^2, *RMSE*, and *MAE* for the random forest model is 0.804, 0.974 and 1.032 respectively. The poorest performance was observed from the linear regression.

Based on the results presented in Tables 4 and it is evident that the BP neural network model exhibits the highest R^2 value of 0.874,

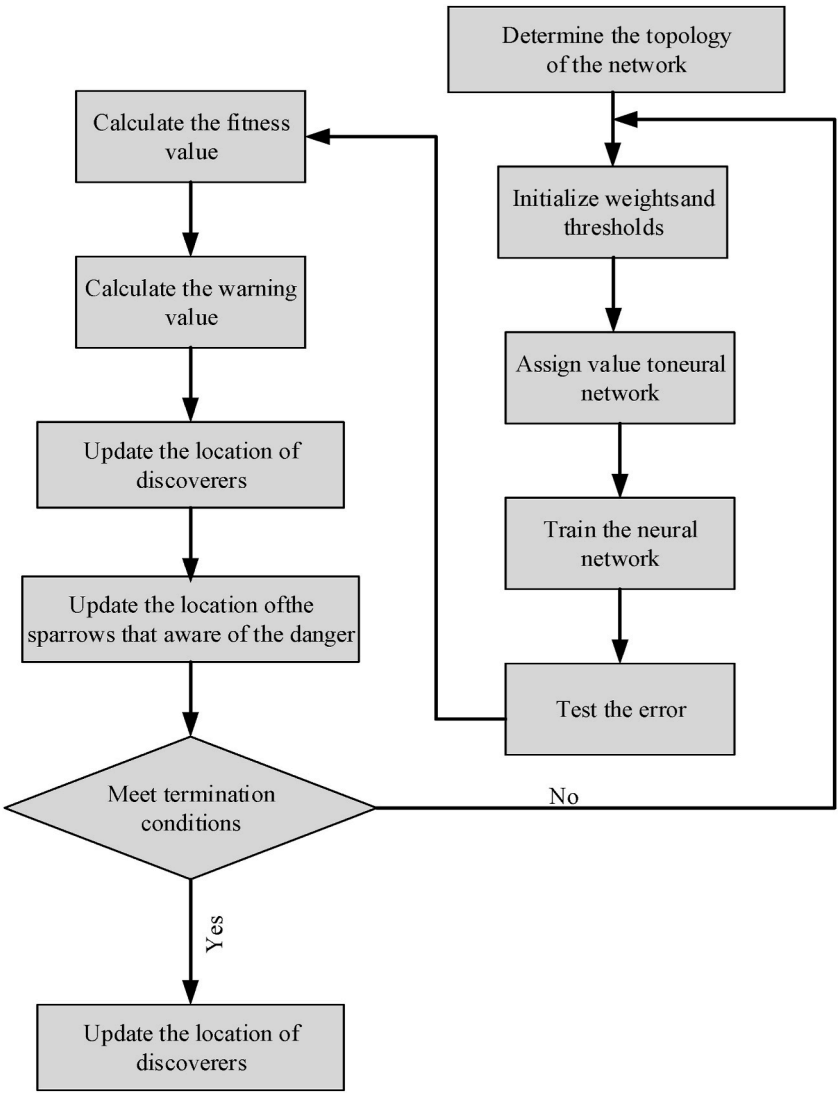

Fig. 11. The calculation process of the BP model updated by SSA.

indicating a strong ability to simulate the variables D and C_s. Furthermore, this model demonstrates the lowest *RMSE* value of 0.835, suggesting that its predictions are relatively close to the actual values. These findings indicate that the BP neural network model performs well in capturing the relationships within the data. Similarly, the random forest model yields an R^2 value of 0.804, indicating a good fit to the data. In contrast, the linear regression model displays the poorest performance among the evaluated models.

The BP neural network model, despite being the top performer in terms of R^2 and *RMSE*, has limitations such as the possibility of getting stuck in local minima and poor stability. To address these issues, the sparrow search algorithm (SSA) was introduced as an advanced method with stronger search capabilities and faster convergence. Not only does SSA aim to improve the accuracy of the BP model, but it also enhances computational speed [26]. The (SSA) incorporates three main components: exploration, exploitation, and learning. During the exploration phase, sparrows explore the search space to discover new regions and potential solutions. In the exploitation phase, sparrows focus on refining promising solutions found during exploration. The learning component allows sparrows to share information and knowledge with each other, facilitating collective learning and improving the overall search process. The implementation of SSA involves several specific steps, which are illustrated in Fig. 11. The updated BP model with SSA can be divided into three parts: the input layer, hidden layer, and output layer. Similar to the BP model, the number of hidden layers, the number of neurons, and the activation function are the same. By incorporating the SSA algorithm into the BP neural network model, both the accuracy of predictions and the computational efficiency can be enhanced, addressing the limitations of the original BP model.

The performance of the BP model and the SSA-BP model is depicted in Figs. 12 and 13, respectively. The results indicate that the BP model requires 16 iterations to converge, while the updated SSA-BP model achieves convergence in only 5 iterations. Moreover, the updated model exhibits a significantly improved root-mean-square error (*RMSE*) of approximately 0.02, which is substantially smaller than that of the BP model. Furthermore, Fig. 14 illustrates the comparison between the test results and the predicted results obtained from the SSA-BP model. The results demonstrate that the SSA-BP model effectively simulates the variables D and C_s, with relative errors ranging from 4.3 % to 11.2 %. This indicates that the model provides accurate predictions in relation to the actual data. To assess the robustness of the models, both the BP model and the SSA-BP model were trained 20 times. The simulated results are presented in Fig. 15. It can be observed that the coefficient of variation for the BP model is considerably larger, ranging from 6 % to 35 %. Conversely, the SSA-BP model exhibits a smaller coefficient of variation, ranging from 5 % to 15 %. This suggests that the neural network optimized by the SSA algorithm not only achieves relatively lower error rates but also demonstrates greater robustness in its predictions. Overall, the findings indicate that the SSA-BP model outperforms the standard BP model, offering improved convergence speed, smaller errors (*RMSE*), and enhanced robustness in its predictions.

The simulated results of SSA-BP model are shown in Figs. 16 and 17, which display the simulated results of D and C_s, respectively. Upon comparing these results with the experimental data, it becomes evident that the predicted values closely align with the test results. The root mean square error (*RMSE*) for D and C_s is calculated. The residual value (*RMSE*) for the D and C_s is 0.978 and 1.232 respectively.

3.2.3. *The influence of each input on D and Cs affected by each input*

To analyze the influence of each parameter on the diffusion coefficient of chloride ions (D) and surface chloride concentration (C_s), the weights between the input layer, hidden layer, and output layer were examined. The corresponding results are presented in Table 5 and Table 6.

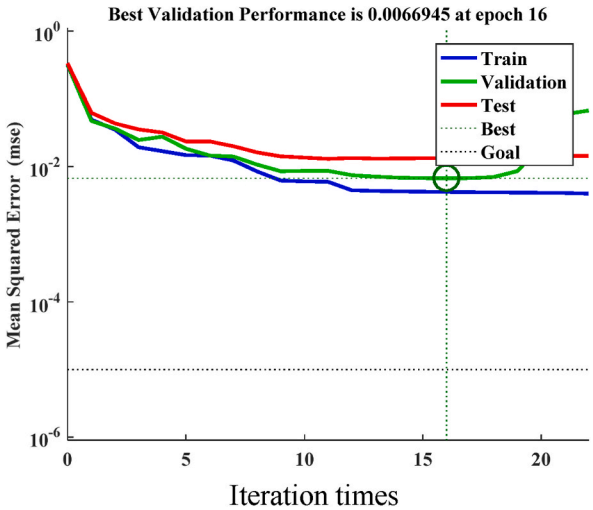

Fig. 12. The performance of BP model.

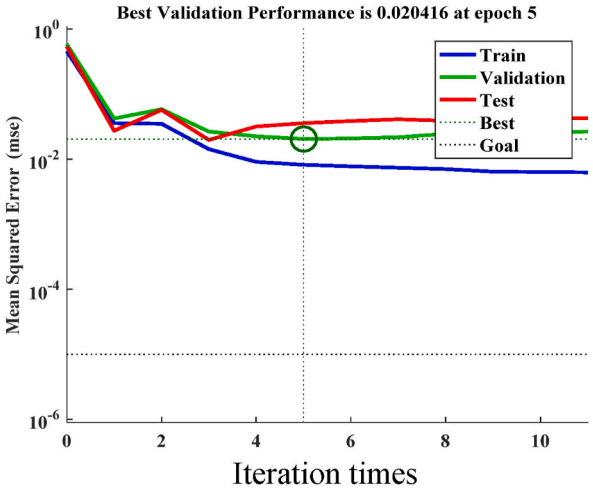

Fig. 13. The performance of SSA-BP model.

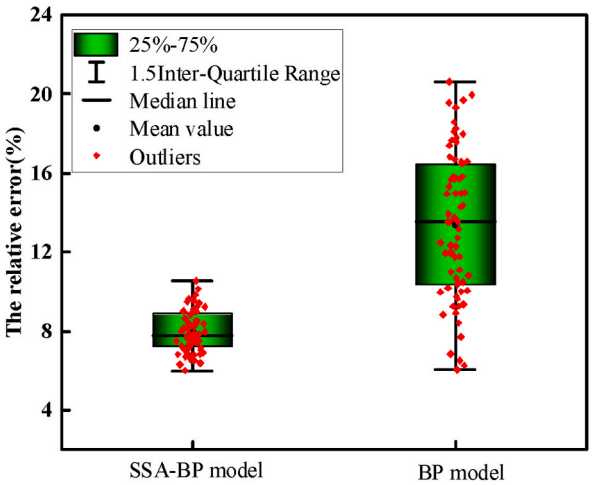

Fig. 14. The relative error.

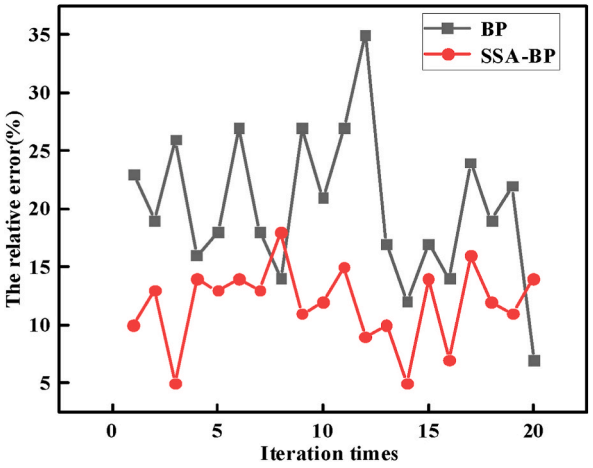

Fig. 15. The comparison results of BP model and SSA-BP model.

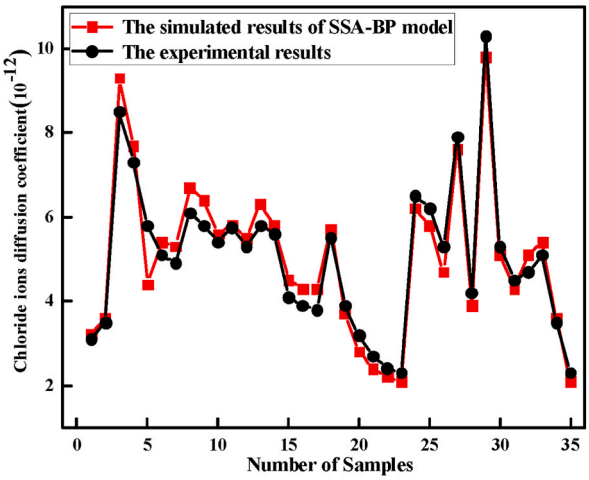

Fig. 16. The comparison results of *D*.

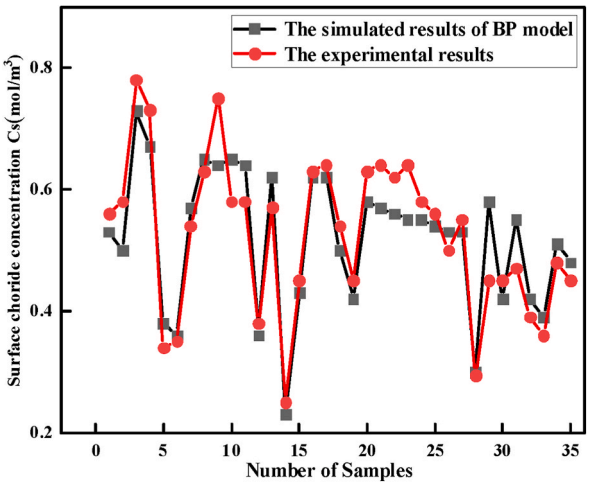

Fig. 17. The comparison results of C_s.

Table 5
Connection weights between the input layer and the hidden layer.

Hidden layer	v	t/t_0	h/h_0	W/C	T/T_0	Bias
B1	−0.06	−0.13	−0.38	−0.15	0.10	−0.04
B2	−0.34	0.90	0.27	0.31	0.88	0.07
B3	−0.70	−0.22	−0.01	−0.34	−0.15	−0.63
B4	0.22	0.13	0.52	−0.22	−0.05	−0.52
B5	0.53	−0.28	0.12	0.64	−0.05	−0.27
B6	−0.24	0.07	0.38	−0.59	0.07	0.42
B7	−0.35	0.11	−0.27	−0.19	−0.34	0.28
B8	0.51	−0.08	−0.32	0.62	−0.58	−0.47
B9	0.45	−0.57	−0.33	−1.08	0.85	−0.02
B10	−0.69	0.21	−0.47	0.54	0.09	−0.41

Table 6
Connection weights of the hidden layer and the output layer.

B1	B2	B3	B4	B5	B6	B7	B8	B9	B10	Bias
−0.51	0.42	0.38	0.55	−0.43	−0.32	−1.32	1.05	0.14	0.38	−0.64

The importance of each factor on the estimated parameters (D and C_s) can be calculated by Eq. (4), which can be expressed as follows [24].

$$Z_{ik}=\frac{\sum_{j=1}^{L}\left(\frac{w_{ij}}{\sum_{r=1}^{N}w_{rj}}v_{jk}\right)}{\sum_{i=1}^{N}\left(\sum_{j=1}^{L}\left(\frac{w_{ij}}{\sum_{r=1}^{N}w_{rj}}v_{jk}\right)\right)} \tag{4}$$

Where $\sum_{r=1}^{N}w_{rj}$ is the sum of the connection weights between the N input neurons and the hidden neuron j, and v_{jk} is connection weight between the hidden neuron j and the output neuron K.

Based on the above steps, the effect of each input on the C_s and D can be achieved the calculation results are shown in Figs. 18 and 19. It can be observed that the most influential factor affecting the diffusion coefficient (D) and surface chloride concentration (C_s) is v. This implies that the parameter v has the strongest impact on the predicted values of D and C_s. Following v, the factors W/C and t/t_0 are identified as significant factors that influence D and C_s. These parameters contribute to the prediction of D and C_s, although to a slightly lesser extent compared to v. Additionally, the parameters T/T_0 and h/h_0 are found to have relatively smaller effects on the diffusion coefficient and surface chloride concentration.

3.2.4. Model established

Based on the updated model and considering the influence of the factors mentioned earlier, two functions have been proposed for estimating C_s (surface chloride concentration) and D (diffusion coefficient). These functions can be expressed as follows:

$$D=10.32\left(\frac{W}{C}\right)^{0.64}\left(\frac{t}{t_0}\right)^{-0.42}\left(\frac{T}{T_0}\right)^{0.32}\left(\frac{h}{h_c}\right)^{0.47}(v)^{-0.81}\times 10^{-12} \tag{5}$$

$$Cs=0.785\left(\frac{W}{C}\right)^{0.72}\left(\frac{t}{t_0}\right)^{0.38}\left(\frac{T}{T_0}\right)^{0.36}\left(\frac{h}{h_c}\right)^{-0.43}(v)^{-0.74} \tag{6}$$

Based on the above steps, the prediction model for estimating the chloride ions concentration at each depth in plain concrete can be written as follows:

$$\left.\begin{aligned} C(x,t)&=C_S\left(1-erf\frac{x}{2\sqrt{D\times t}}\right)\\ D&=10.32\left(\frac{W}{C}\right)^{0.64}\left(\frac{t}{t_0}\right)^{-0.42}\left(\frac{T}{T_0}\right)^{0.32}\left(\frac{h}{h_c}\right)^{0.47}(v)^{-0.81}\times 10^{-12}\\ C_s&=0.585\left(\frac{W}{C}\right)^{0.72}\left(\frac{t}{t_0}\right)^{0.38}\left(\frac{T}{T_0}\right)^{0.36}\left(\frac{h}{h_c}\right)^{-0.43}(v)^{-0.74} \end{aligned}\right\} \tag{7}$$

As described in Eq. (7), it is observed that both the diffusion coefficient (D) and surface chloride concentration (C_s) tend to increase with an increase in the water-cement ratio (W/C), the ratio of the temperature (T/T_0). Conversely, the coarse aggregate volume fraction (v) is negatively correlated with D and C_s. In addition, Several factors contribute to this phenomenon: Increased porosity: An increase in the water-cement ratio leads to higher porosity in concrete specimens. This increased porosity allows for easier diffusion of

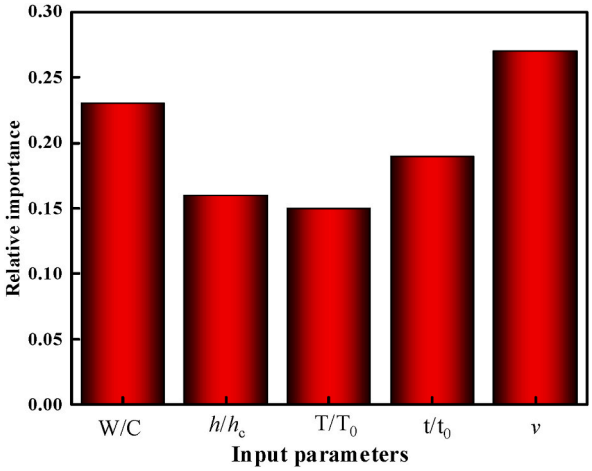

Fig. 18. The influence of each parameter on the chloride ions diffusion coefficient.

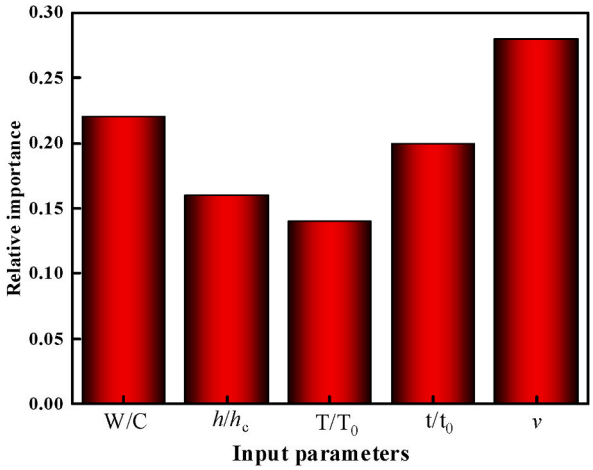

Fig. 19. The influence of each parameter on the surface chloride ions concentration.

chloride ions, resulting in an increase in the diffusion coefficient (D) [27]. Temperature effects: In high-temperature environments, it can not only accelerate the thermal motion of the chloride ions but also can improve the chemical combination capacity of the chloride ions. Humidity effects: Higher humidity can increase the moisture content in concrete, leading to a higher internal moisture level and increased saturation of pores. This, in turn, accelerates the diffusion rate of chloride ions in concrete, resulting in an increase in the chloride ion diffusion coefficient. Blocking effect of coarse aggregate: Studies have indicated that the coarse aggregate volume fraction (v) can have a blocking effect on the diffusion of chloride ions. As the volume fraction of coarse aggregate increases, the pathways for chloride ion diffusion become more restricted, resulting in a decrease in the diffusion coefficient (D) and surface chloride concentration (C_s).

To validate the accuracy of the proposed model, the test results from the control group were used for comparison. The comparison results are presented in Table 7 which indicate a close agreement between the predicted and experimental values, with a maximum relative error of 21.1 %. However, several factors should be taken into consideration to improve and update the proposed model.

(1) Microstructure consideration: The current model does not account for the underlying microstructure of the material itself. Increasing the water-cement ratio (W/C) and coarse aggregate volume fraction (v) can lead to higher porosity in the concrete, which may accelerate chloride ion diffusion. Incorporating the effects of microstructure on the diffusion process could enhance the accuracy of the model.
(2) Influence of micro-cracks: The surface chloride concentration (C_s) and diffusion coefficient (D) are often influenced by micro-cracks on the concrete specimens. However, incorporating this factor into the model is challenging due to the random distribution of cracks.
(3) Expansion of the database: The accuracy of the prediction model is heavily dependent on the number of available test data. To enhance the robustness and reliability of the model, it is recommended to expand the database by including more experimental data from various sources or conducting additional experiments.

To further validate the model's accuracy, a subset of datasets was selected from studies in Literature 8 and Literature 9. Literature 8 and Literature 9 explored the time-varying behavior of chloride ions in concrete structures based on accelerated artificial experiments. The chloride ion concentration in the corrosive environment was 3.5 %, with a water-cement ratio of 0.54. Using this model, the chloride ion concentration at different erosion depths in concrete was calculated and compared with experimental test results. The comparison results are shown in Fig. 20.

As shown in Fig. 20, the predicted results are relatively close to the actual results, with the relative error within 15 %. This indicates that the prediction model can accurately forecast the chloride ion concentration among the various layers of concrete and can intuitively reveal the transmission pattern of chloride ions in concrete structures.

Table 7
The comparison results between the experiment and the simulated results.

W/C	t/t_0	h/h_0	v	T/T_0	relative error
0.30	1.25	1.00	0.30	1.00	4.5 %
0.35	2.32	1.03	0.31	1.20	8.9 %
0.45	3.57	1.05	0.32	1.40	14.1 %
0.50	7.14	1.10	0.33	1.60	17.6 %
0.60	8.40	1.15	0.34	1.80	21.1 %

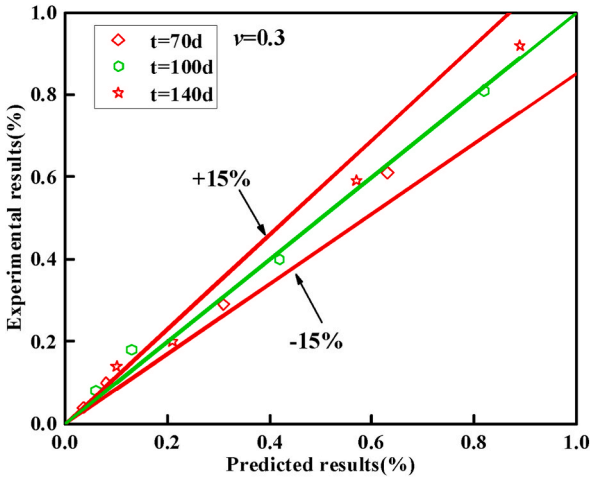

Fig. 20. Comparison results between the experimental results and predicted results.

Table 8
The previous models.

Literature	Previous models
P. S Mangat [29]	$\begin{cases} C(x,t) = C_S\left(1 - erf\dfrac{x}{2\sqrt{D \times t}}\right) \\ D = D_0\left(\dfrac{t_0}{t}\right)^m m = 2.5 \times (W/B) - 0.6 \\ C_S(t) = 1.5\left[1 - erf\left(\dfrac{x}{2\sqrt{\dfrac{5.736 \times 10^{-5}}{0.56}t^{0.56}}}\right)\right] \\ D_0 = 7.08 \times 10^{-5} \times t^{-0.44} \end{cases}$
Wang [8]	$\begin{cases} C(x,t) = C_S\left(1 - erf\dfrac{x}{2\sqrt{D \times t}}\right) \\ C_S(t) = 0.00027t + 0.5939 \\ D = D_{ref} \times f_1(t) \times f_2(v) \times f_3(s) \\ D_{ref} = 5.259 \times 10^{-12} m^2/s, f_1(t) = \left(\dfrac{t_{ref}}{t}\right)^{\alpha}, \alpha = 0.3187 \\ f_2(v) = 1.6902 - 1.3804v, f_s(s) = 0.0019s^2 - 0.1456s + 3.6899 \end{cases}$
Ju [30]	$\begin{cases} C(x,t) = C_S\left(1 - erf\dfrac{x}{2\sqrt{D \times t}}\right) \\ C_S(t) = 0.096t - 0.048 \\ D = D_0\left(\dfrac{t_0}{t}\right)^m \\ D_0 = 6.12 \times 10^{-12} m^2/s \\ f_1(t) = \left(\dfrac{t_{ref}}{t}\right)^{\alpha}, \alpha = 0.22 \end{cases}$
Hu [29]	$\begin{cases} C(x,t) = C_S\left(1 - erf\dfrac{x}{2\sqrt{D \times t}}\right) \\ C_S(t) = 0.00027t + 0.5939 \\ D = \dfrac{2.14 \times 10^{-10} V_p^{2.75}}{V_p^{1.75}(3 - V_p) + 14.44(1 - V_p)^{2.75}} \\ V_p = \dfrac{w/c - 0.17\alpha}{w/c + 0.32}, \alpha = 1 - [\exp - 3.15(w/c)] \\ C_S(d) = 0.127\%, d < 0.10 \\ C_S(d) = 0.05\% - 0.078 \lg d, C_S(d) = 0.123\% \end{cases}$

Table 9
The statistical measures of the above models.

Prediction model	$C_i(x,t)/C(x,t)$	The relative error	R_{MSE}
P. S Mangat	1.67	62.7 %	3.683
Wang	1.38	42.8 %	3.132
Ju	0.79	30.2 %	2.876
Hu	1.42	51.3 %	3.432
Proposed model	1.18	12.1 %	1.264

3.2.5. *Model validation with previous models*

Currently, several models have been developed to investigate the chloride ion concentration at various depths in concrete structures, as presented in Table 8. The accuracy and goodness of fit were evaluated using metrics such as root mean square error (*RMSE*), relative error, as shown in Table 9. The results demonstrate that the models proposed by P. S Mangat [28], Wang [8], and Hu [29] are overly conservative, with predicted results consistently higher than the experimental data. In particular, the model proposed by P. S Mangat exhibits a ratio of the average value of $Ci(x,t)/C(x,t)$ of 1.67, the largest relative error (62.7 %), and a high *RMSE* value of 3.683. Conversely, the model established by Ju [30] consistently underestimates the experimental results, with a relative error of 30.2 % and an *RMSE* value of 2.876. In contrast, the model proposed in this paper demonstrates good performance in predicting the chloride ion concentration at each depth. It exhibits the lowest relative error (12.1 %) and *RMSE* (1.264) among the compared models. These findings suggest that the proposed model can effectively estimate the chloride ion concentration at various depths in concrete structures.

3.3. *A prediction model for estimating the service life of reinforced concrete structures*

According to previous studies, the steel bar starts to rust when the chloride ion concentration on the steel bar surface reaches the critical value of its debuffing. The concrete protective layer was lost, leading to structural failure. A conservative method for estimating the service life of RC structures shows that cracking of the concrete cover commences shortly when the reinforcement starts to rust. Therefore, the initial corrosion time of the reinforcement and cracking time of the concrete protective layer should be used as the basis for evaluating the service life of RC structures [30].

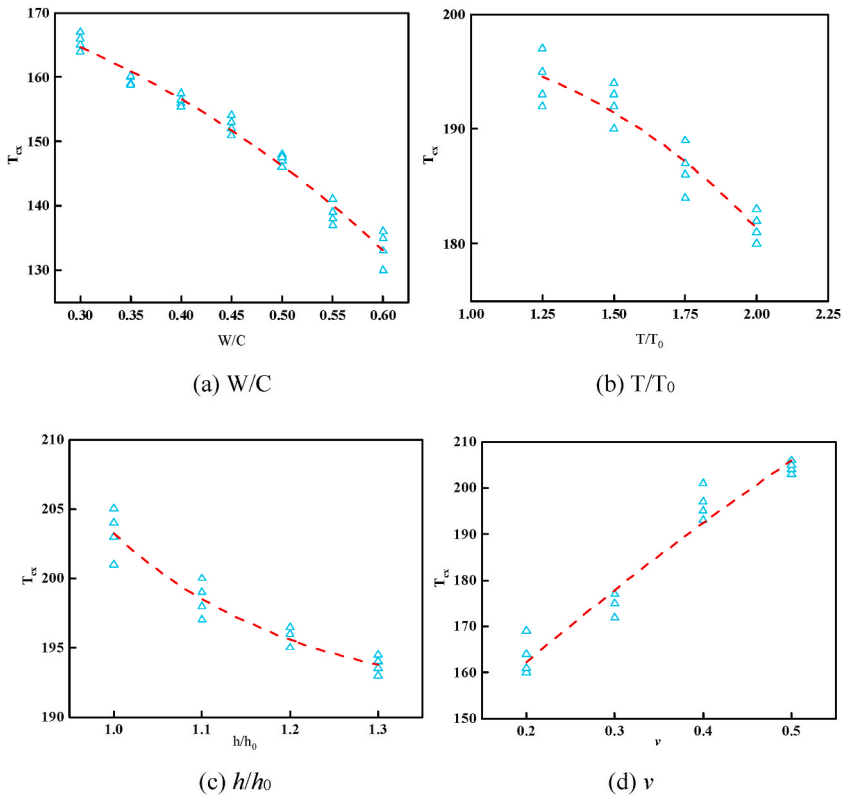

Fig. 21. The initial corrosion time of reinforcement affected by each input.

3.3.1. The initial corrosion time of steel bar

According to the Design and Construction Guide for Durability of Concrete Structures (CCES01-2004), the critical value of chloride ion concentration in reinforced concrete (RC) members affected by corrosion in the marine tidal zone is specified as 0.8 % [30]. This critical value represents the percentage of chloride ion content in cementitious materials. In this study, to determine the mass fraction of chloride ion content in concrete materials, the mix proportions of the specimens were considered. By converting the percentage value of chloride ion content in cementitious materials to the corresponding mass fraction, you can accurately assess the chloride ion concentration in the concrete specimens.

By substituting the critical value of the chloride ion concentration into Eq. (7) with a specific depth ($x = 20$ mm), the impact of each input variable on the initial corrosion time T_{cx} (days) of the reinforcement within the concrete structures can be determined. The results are presented in Fig. 21. The blue dots represent the initial corrosion time of the steel bars under different conditions, and the red curve is fitted through these blue dots to describe the impact of each input variable on the initial rusting time of the steel bars. It can be concluded that an increase in the (W/C), (T/T_0), and (h/h_0) leads to a decrease in the initial corrosion time of reinforcement.

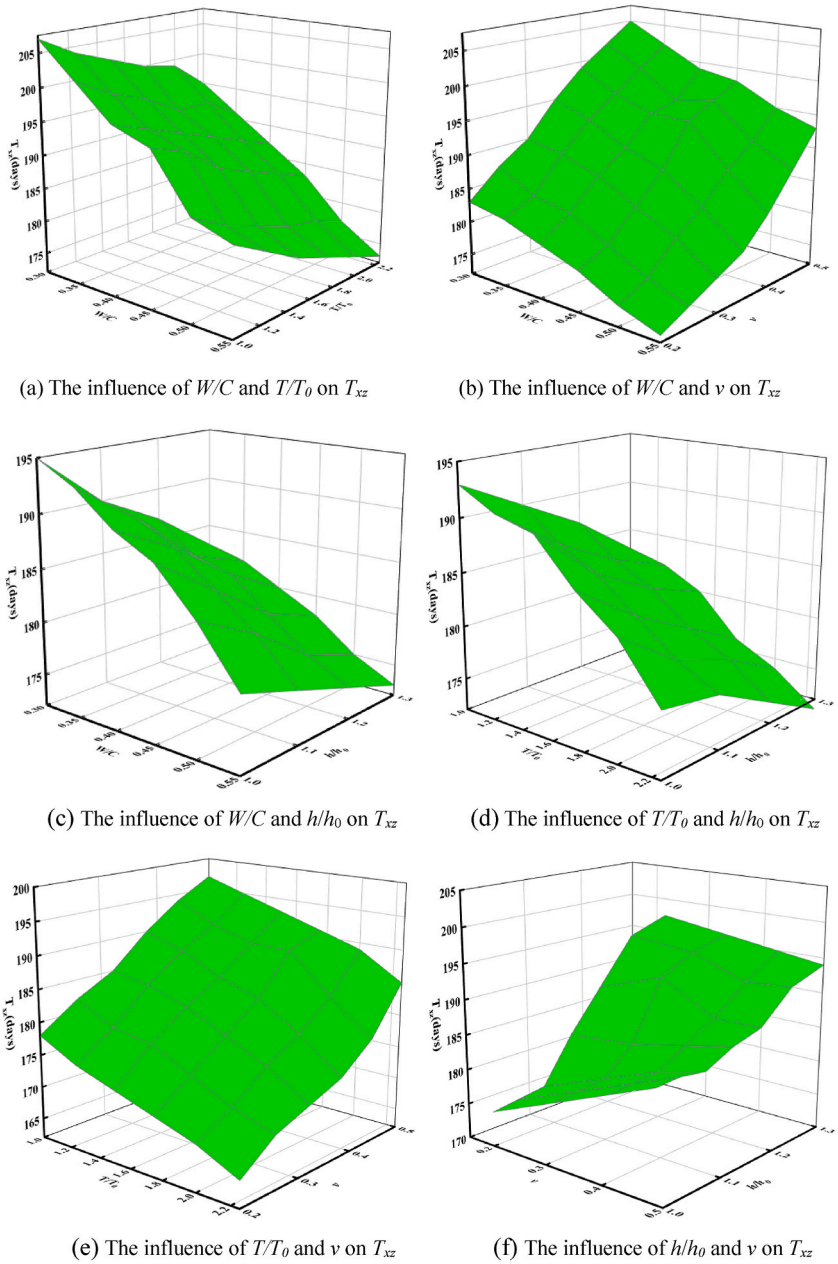

Fig. 22. The influence of each input on the T_{xz}.

Conversely, as the (v) increases, the initial corrosion time tends to increase. The influence of the water-to-cement ratio (W/C) and the volume fraction of coarse aggregates (v) on the initial corrosion of reinforcement is particularly significant. As the W/C ratio increases from 0.3 to 0.6, the initial corrosion time of reinforcement decreases by 21.8 %. Similarly, when the volume fraction of coarse aggregates (v) changes from 0.2 to 0.5, the initial corrosion time of reinforcement increases by 25.8 %.

While the effects of (T/T_0) and (h/h_0) on it are relatively limited, with variations in the initial rusting time of the steel within 10 %. These trends highlight the significant impact of W/C, T/T_0, h/h_0, and v on the corrosion process of reinforced concrete structures, emphasizing the importance of considering these factors in corrosion prevention and mitigation strategies.

3.3.2. Cracking time of concrete cover

Eq. (8) was used to predict the service life of the structure, which can be expressed as follows [31]:

$$\delta_{cr} = \int_0^{T_{xz}} \lambda(t)dt \tag{8}$$

Where: δ_{cr} means the critical depth of steel bar, which can be calculated by Eq (9) [31]. $\lambda(t)$ is a time-dependent function of the corrosion rate of the steel bars, and the relationship between them can be found in Eq. (10) [31]. T_{xz} refers to the service life of a structure.

$$\delta_{cr} = 0.012\frac{M}{d} + 0.00084f_{cuk} + 0.018 \tag{9}$$

$$\lambda(t) = 0.0116 \times \frac{37.8(1 - W/C)^{-1.64}}{M} \times 0.85t^{-0.29} \tag{10}$$

Substituting Eq (9) and Eq (10) into Eq (8), T_{xz} can be written as follows:

$$T_{xz} = \left\{ \frac{M \times \left[0.0228 \times \left(\frac{M}{d}\right) + 0.0016 \times f_{cuk} + 0.0343\right]}{(1 - W/C)^{-1.64}} \right\}^{1.4} \tag{11}$$

Where: M denotes the thickness of the concrete cover, d denotes the diameter of the steel bar (M = 20 cm) and f_{cuk} denotes the compression strength of specimens after corrosion (the compressive strength of concrete varies under different environmental conditions). From the above steps, the cracking time of concrete cover of reinforced concrete structures with different corrosion degrees can be obtained, some calculated results are shown in Fig. 22(a)-(f). The results show that the W/C , T/T_0 , h/h_0 both have a negative effect on T_{xz}. With the W/C , T/T_0 , h/h_0 increase, which will result in decreasing the T_{xz}. But for the v, as the v increases, the T_{xz} increases. In addition, the water-to-cement ratio and the volume fraction of coarse aggregates have a significant impact on the cracking time of concrete cover, while the remaining input variables have relatively minor effects.

3.3.3. The service life of reinforced concrete structures

Based on the aforementioned steps, the service life of reinforced concrete structure T_{sm} can be expressed as $T_{sm} = T_{cx} + T_{xz}$. Some results are listed in Table 10. As shown in Table 10, the volume fraction of coarse aggregate has the most significant impact on the service life of reinforced concrete structures. Increasing the volume fraction of coarse aggregate slows down the erosion caused by chloride ions, resulting in a significant improvement in the structure's service life. Following that, the water-cement ratio becomes a crucial factor. A higher water-cement ratio increases the porosity of the concrete structure, accelerating the diffusion of chloride ions and consequently reducing the service life of the reinforced concrete structure, leading to structural deterioration. In addition to these factors, the service life of reinforced concrete structures can also be influenced by environmental factors such as temperature and humidity, although their impact is relatively less pronounced.

To further demonstrate the accuracy of this model's predictions, corresponding experimental studies on reinforced concrete structures were conducted in an artificially accelerated corrosion environment. Fig. 23 shows the corrosion loss of reinforced concrete

Table 10
The calculation results of T_{sm}.

W/C	T/T$_0$	h/h_0	v	T_{sm} (days)
0.6	1.25	1.00	0.2	173
0.5	1.50	1.00	0.2	177
0.3	1.50	1.10	0.4	191
0.4	1.75	1.20	0.2	183
0.4	1.75	1.20	0.3	179
0.4	1.75	1.20	0.5	206
0.5	2.00	1.30	0.2	168
0.5	2.00	1.30	0.3	194
0.3	2.25	1.30	0.5	217
0.6	1.25	1.00	0.3	185

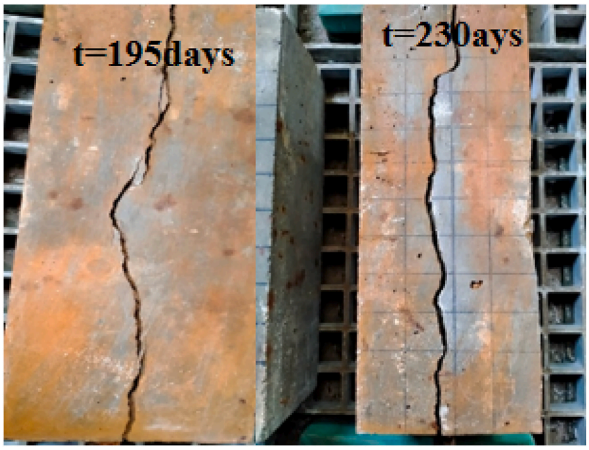

Fig. 23. Corrosion status of reinforced concrete structures.

structures at 194 days and 230 days, respectively. The results indicate that when the reinforced concrete corrodes for 195 days in an artificially accelerated environment, penetrating cracks appear on the concrete surface, with relatively small crack widths at this stage. However, after 230 days of corrosion, the crack width significantly increases, and the internal steel reinforcement also exhibits extensive corrosion damage.

Although this section has established a predictive model for the lifespan of reinforced concrete structures and obtained lifespan predictions under various conditions, there are still some shortcomings in the model. First, in the process of calculating the lifespan of reinforced concrete structures, it is assumed that once the steel reinforcement corrodes and causes the concrete surface to crack, the reinforced concrete structure fails. However, in reality, reinforced concrete still retains a certain load-bearing capacity when it cracks due to steel corrosion, making the model's predictions somewhat conservative. Second, the model can only assess the service condition of reinforced concrete structures in artificially accelerated corrosive environments and does not fully reflect the decay pattern of their lifespan in actual service environments. The deterioration of reinforced concrete structures in real service environments is a relatively slow process, with lifespans extending over several decades. Accurately simulating the rusting process of reinforced concrete is both time-consuming and extremely difficult. Therefore, in future research, it is necessary to establish an equivalent loss conversion relationship between the artificially accelerated corrosive environment and the service environment to better predict their lifespan in actual service conditions.

4. Conclusion

This paper conducted a physical test to evaluate the concentration of chloride ions at various depths in plain concrete structures. Moreover, using the principles of the second Fick's law, a prediction model was developed to understand the diffusion behavior of chloride ions within plain concrete. The model takes into account the combined influence of random factors related to both materials and environmental conditions. In addition, this study analyzed the service life of reinforced concrete structures. The following conclusions were drawn from the research.

(1) A physical test was conducted to investigate the diffusion behavior of chloride ions in plain concrete. The results revealed that the W/C, (T/T_0) and (h/h_0) all positively affect the diffusion of chloride ions. This means that as these factors increase, the rate of chloride ion diffusion also increases. On the other hand, the v has a blocking effect on the diffusion of chloride ions. These findings provide valuable insights into the mechanisms of chloride ion diffusion in plain concrete. By understanding the positive effects of the water-cement ratio, temperature, and humidity, as well as the blocking effect of v, strategies can be developed to control and mitigate the diffusion of chloride ions in reinforced concrete structures.

(2) An updated model was proposed to predict the diffusion coefficient (D) and surface chloride concentration (C_s) in concrete structures. This model utilized a BP Neural Network that was improved by the Sparrow Search Algorithm (SSA). Compared to previous models, the results demonstrated significant improvements. The neural network optimized by SSA exhibited not only a relatively small error in predicting D and C_s but also demonstrated enhanced robustness. The utilization of SSA in optimizing the neural network allowed for more accurate predictions and improved the overall performance of the model. The enhanced robustness suggests that the model is capable of providing reliable predictions even when confronted with varying input conditions or uncertainties.

(3) A study on the importance of the input features employed in the BPNN algorithm by SSA revealed that the water-cement ratio and the volume of coarse aggregate fraction are considered as the most critical factors affecting the diffusion coefficient (D) and the (C_s). This research sheds light on the importance of these specific input features in accurately predicting and understanding the behavior of chloride ions in concrete structures.

(4) Based on Fick's second law, this study presents a novel prediction model for estimating chloride ion concentration at various depths within concrete structures. The model takes into account the coupled effects of both materials and the surrounding

environment. Comparative analysis with the previous model and experimental results reveals that the results obtained from the proposed model in this paper closely align with the experimental data, indicating a significant improvement over previous approaches.

(5) The service life of reinforced concrete structures was analyzed, taking into account the coupled effects of both materials and the surrounding environment. The results highlight the significance of the volume fraction of coarse aggregate in determining the service life. It was observed that increasing the volume fraction of coarse aggregate has a notable impact on slowing down the erosion caused by chloride ions, thereby improving the service life of the structure. Furthermore, the water-cement ratio was identified as a crucial factor affecting the service life. A higher water-cement ratio leads to increased porosity in the concrete structure, facilitating the diffusion of chloride ions and subsequently reducing the service life. While environmental factors such as temperature and humidity can also influence the service life of reinforced concrete structures, their effects are relatively less pronounced compared to the volume fraction of coarse aggregate and water-cement ratio. Nonetheless, considering these environmental factors alongside material properties is essential for a comprehensive assessment of the structure's durability and longevity.

(6) Additionally, in subsequent research, in order to more accurately predict the durability and lifespan of reinforced concrete structures, a three-dimensional diffusion model should be developed to describe the diffusion pattern of chloride ions in concrete structures.

CRediT authorship contribution statement

XuanRui Yu: Writing – original draft, Validation, Software, Methodology, Investigation, Formal analysis, Data curation, Conceptualization. **Jiehong Li:** Writing – review & editing, Software, Project administration, Methodology, Investigation, Conceptualization. **Yang Yu:** Writing – review & editing, Software, Funding acquisition. **An Xiang Song:** Writing – review & editing, Validation, Methodology.

Declaration of competing interest

The authors declare that they have no known competing financial interests or personal relationships that could have appeared to influence the work reported in this paper.

Data availability

Data will be made available on request.

Acknowledgments

This research was partially supported by the Australian Research Council (Grant No. IH150100006). The authors would like to express their gratitude for the financial support provided by the funding body.

References

[1] J. Wang, L. Yang, J. Zhao, Q. Ma, B. Yu, Modelling and verification for dual time-dependent chloride diffusion of circular concrete columns in marine environment, J. Build. Eng. 76 (2023) 107149.
[2] S. Yan, Y. Liang, Fractal derivative model with time dependent diffusion coefficient for chloride diffusion in concrete, J. Build. Eng. (2023) 106897, 2023, 74.
[3] L. Yu, H. Chu, Z. Zhu, L. Jiang, H. Dong, Determination of the chloride ion content in concrete under simultaneous chloride and sulphate ion attack, J. Build. Eng. 72 (2023) 106579.
[4] B. Larbi, W. Dridi, P. Dangla, P Le Bescop, Link between microstructure and tritiated water diffusivity in mortars: impact of aggregates, Cement Concr. Res. (82) (2016) 92–99.
[5] A. M D, Thomas P.B. Bamforth, Modeling chloride diffusion in concrete effect of fly ash and slag, Cement Concr. Res. (4) (1999) 487–495.
[6] Marcialisa Collepardim, Turrizianir, Penetration of chloride ions into cement pastes and concretes, J. Am. Ceram. Soc. 55 (10) (1972) 534–535.
[7] J.J. Zheng, X.Z. Zhou, Prediction of the chloride diffusion coefficient ofconcrete, Mater. Struct. 40 (7) (2006) 693–701.
[8] Y.Z. Wang, X.L. Gong, L.J. Wu, Prediction model of chloride diffusion in concrete considering the coupling effects of coarse aggregate and steel reinforcement exposed to marine tidal environment, Construct. Build. Mater. 216 (2019) 40–57.
[9] Y. Wang, C. Liu, Y. Wang, et al., Time-and-depth-dependent model of chloride diffusion coefficient for concrete members considering the effect of Coarse aggregate, J. Mater. Civ. Eng. 30 (3) (2018) 1–12.
[10] H. Yu, R.J. Himiob, W.H. Hartt, Effects of reinforcement and coarse aggregateson chloride ingress into concrete and time-to-corrosion: Part 1-Spatial chloride distribution and implications, Corrosion 63 (9) (2007) 843–849.
[11] H. Yu, R.J. Himiob, W.H. Hartt, Effects of reinforcement and coarse aggregateson chloride ingress into concrete and time-to-corrosion: Part 2-Spatialdistribution of coarse aggregates, Corrosion 63 (10) (2007) 924–931.
[12] L. Liu, D. Shen, H. Chen, et al., Aggregate shape effect on the diffusivity ofmortar: a 3D numerical investigation by random packing models of ellipsoidalparticles and of convex polyhedral particles, Comput. Struct. 144 (2014) 40–51.
[13] A.K. Suryavanshi, J.D. Scantlebury, S.B. Lyon, Corrosion of reinforcement steel embedded in high water-cement ratio concrete contaminated with chloride, Cement Concr. Compos. 20 (4) (1998) 263–281.
[14] Z. Ren, L.Z. Xiao, W.C. Shi, Experimental study and numerical analysis on chloride diffusion coefficient of concrete with various water-cement ratios, Key Eng. Mater. 726 (2017) 547–552.
[15] J.L. Liu, Z. Fang, New method for calculating chloride diffusion in concrete under multi-factors, J. Build. Mater. 16 (5) (2013) 777–781.
[16] E.J. Hansen, V.E. Saouma, Numerical simulation of reinforced concrete deterioration: Part I: chloride diffusion, ACI Mater. J. 96 (2) (1999) 173–180.
[17] S.W. Hu, X. Jian, et al., Influences of time, temperature, and humidity on chloride diffusivity: mesoscopic numerical research, J. Mater. Civ. Eng. 29 (11) (2017) 237–248.

[18] O.A. Hodhod, H.I. Ahmed, Developing an artificial neural network model to evaluate chloride diffusivity in high performance concrete, HBRC Journal 9 (1) (2013) 15–21.
[19] Y.Y. Kim, B.J. Lee, S.J. Kwon, Evaluation technique of chloride penetration using apparent diffusion coefficient and neural network algorithm, Adv. Mater. Sci. Eng. 9 (11) (2014) 1–13.
[20] M. Al-samawi, J. Zhu, W. Rong, Application of 3D cellular automata-based analysis to chloride diffusion process in concrete bridges, Structures 47 (2023) 500–519.
[21] D. Kim, H. Lee, S. Lee, et al., A study on the evaluation of probabilistic durability life for RC structures deteriorated by chloride ion, Key Eng. Mater. 348–349 (2007) 417–420.
[22] T. Gupta, K.A. Patel, S. Siddique, R.K. Sharma, S. Chaudhary, Prediction of mechanical properties of rubberized concrete exposed to elevated temperature using ANN[J], Measurement. 147 (5) (2019) 106870.
[23] Y.Z. Wang, L. Wu, Y. Wang, et al., Effects of coarse aggregates on chloride diffusion coefficients of concrete and interfacial transition zone under experimental drying-wetting cycles, Construct. Build. Mater. 185 (10) (2018) 230–245.
[24] Linjian Wu, Study on Chloride Ion Diffusion Considering the Heterogeneity of Concrete Materials and the Blocking Effect of Reinforcement [D], Tianjin University, 2020 (In Chinese).
[25] X.R. Yu, Developing an artificial neural network model to predict the durability of the RC beam by machine learning approaches, Case Stud. Constr. Mater. 17 (2022) 01382.
[26] Hu, IOP Conf. Ser. Earth Environ. Sci. 719 (2021). Article ID 022028.
[27] L.Y. Li, J. Xia, S.S. Lin, A multi-phase model for predicting the effective diffusion coefficient of chlorides in concrete, Construct. Build. Mater. 1 (26) (2012) 295–301.
[28] P.S. Mangat, B.T. Molloy, Prediction of long term chloride concentration in concrete[J], Mater. Structures 27 (6) (1994) 338.
[29] S.W. Hu, X. Jian, et al., Influences of time, temperature, and humidity onChloride diffusivity: mesoscopic numerical research, J. Mater. Civ. Eng. 29 (11) (2017) 237–248.
[30] X.L. Ju, L.J. Wu, M.W. Liu, et al., Service life prediction of reinforced concrete piers considering chloride ion attack dimension, Materials Guide 35 (24) (2021) 7 (in Chinese).
[31] CCES 01-2004 Guide to Durability Design and Construction of Reinforced Structures, China Architecture and Building Press, China, 2004 (In Chinese).